

Fig. 3 Graphical solution for Eq. (21).

In the improved method, we imagine the fin extended to  $r_{2c}$  such that the temperature gradient will be zero at  $r = r_{2c}$ . The heat flow at  $r = r_2$  is

$$q_{r=r_2} = 4\pi r_2 \delta h \theta_L \quad (19)$$

This quantity of heat must be dissipated through the two surfaces of the extended fin which is given in Eq. (13) by replacing  $r_1$ ,  $r_2$ , and  $\theta_0$  with  $r_2$ ,  $r_{2c}$ , and  $\theta_L$ , respectively. Equating the result to the right side of Eq. (19), we obtain

$$-\delta N = \frac{I_1(Nr_2)K_1(Nr_{2c}) - I(Nr_{2c})K_1(Nr_2)}{I_0(Nr_2)K_1(Nr_{2c}) + I_1(Nr_{2c})K_0(Nr_2)} \quad (20)$$

We now have an equation with one unknown,  $r_{2c}$ , which can be arranged to yield

$$\frac{I_1(Nr_{2c})}{K_1(Nr_{2c})} = \frac{I_1(Nr_2) + \delta N I_0(Nr_2)}{K_1(Nr_2) - \delta N K_0(Nr_2)} \quad (21)$$

with the right side containing functions of known parameters. Equation (21) cannot be solved analytically for  $r_{2c}$ , since  $r_{2c}$  is the argument of the modified Bessel functions. It can be solved, however, by method of iteration to any accuracy desired. A graphical solution of the Eq. (21) is given in Fig. 3. Knowing the values of  $r_2$  and  $\delta$ , the corresponding value of  $r_{2c}$  can be read from the graph. The heat transfer at the root,  $q_{r=r_1}$  of a nonadiabatic radial fin is then obtained by replacing  $r_2$  in Eq. (13) by this value of  $r_{2c}$ . Theoretically, the value of  $q_{r=r_1}$  thus obtained should be identical to that obtained from the exact solution given in Eq. (16).

### Concluding Remarks

This new method for treating the problem of heat conduction through finned surfaces is similar to the approximation method of Harper and Brown,<sup>1</sup> except that the length of the imaginary extended tip is calculated rather than being assumed, and no assumption of uniform temperature of the extended tip is used. Therefore, theoretically, it should lead to exact solutions of the heat conduction through finned surfaces with nonadiabatic tips. The only prerequisite for this method (as for the method of Ref. 1) is the existence of the solution for the case of the finned surface with an adiabatic tip, which is always much easier to obtain.

For the case of a longitudinal fin, an exact solution is obtained, because the simple fin geometry enables us to derive an explicit expression for the imaginary extension length  $\epsilon$ . For the case of a radial fin, solutions are given in graphical form, because  $\epsilon$  is part of the arguments of some modified Bessel functions. One may derive an approximate expression for  $\epsilon$  by expanding those Bessel functions into polynomials. However, the results of heat conduction obtained

by retaining terms up to  $\epsilon^2$  are found<sup>4</sup> to be not much better than those calculated by the method of Harper and Brown.

### References

- Harper, W. B. and Brown, D. R., "Mathematical Equations for Heat Conduction in the Fins of Air Cooled Engines," Rept. 158, 1922, NACA.
- Schneider, P. J., *Conduction Heat Transfer*, 2nd ed., Addison-Wesley, Reading, Mass., 1957, p. 63.
- Kraus, N. W., *Extended Surfaces*, Spartan, Baltimore, 1964.
- Woods, J. J., "An Improved Approximation Method for Predicting the Steady-State Performance of Extended Surfaces with Non-Adiabatic Tips," M.S. thesis, June 1968, Univ. of Delaware.

## A New Concept for Low-Range Pressure Measurements on Full-Scale Flight Re-Entry Vehicles

J. M. CASSANTO\* AND F. C. GEORGE†  
General Electric Company, King of Prussia, Pa.

### Introduction

LOW-RANGE pressure sensors are needed on re-entry test vehicles for base pressure measurements to determine the altitude of onset of boundary-layer transition. Absolute pressure transducers for this purpose tend to be large and bulky because they utilize an evacuated, hermetically sealed reference chamber. Since some leakage occurs even with the best hermetic seals, the reference chamber is made rather large to insure calibration stability and a long shelf life. The new concept<sup>1</sup> described herein avoids these problems by using a differential pressure sensor with a controlled leak rate (time constant) that vents to the vacuum of free space and uses the resultant vacuum as a reference pressure during reentry. The time constant can be made short for normal ballistic re-entry trajectories or extremely long for planetary entry probe missions, thus insuring an accurate, reliable vacuum reference during entry. A vent tube restrictor/feedback loop containing a porous slug of metal with a known leak rate (Fig. 1) produces the time constant.

The concept of a differential pressure transducer with a time constant to measure absolute pressures has been used for years in wind tunnels and shock tunnels<sup>2-4</sup> but the proposed use on flight vehicles is new. In shock-tunnel tests, the differential sensor equalizes to the vacuum conditions in the test section prior to the test. During a short blowdown run, the calibration side of the transducer holds the vacuum long enough to sense the difference between the measured pressure and the vacuum. For the flight application, the time constant is designed so that the vacuum on the reference side holds long enough ( $t \sim 10$  sec.) to make the flight measurement. The flight prototype unit described herein (Fig. 2) employs a shock-tunnel-type (capacitance) transducer, has a range from 0 to 0.2 psid, weighs 6 oz, and has a volume of 6 in.<sup>3</sup> A comparable "off-the-shelf" absolute pressure sensor of equivalent range weighs 9 oz and has a volume of 9 in.<sup>3</sup>

### Powered Flight and Re-Entry Pressure Simulation

For a typical short-duration ballistic flight ( $\sim 340$  sec), atmospheric pressure exists on each side of the diaphragm

Received May 6, 1969; revision received July 7, 1969.

\* Supervising Engineer, Re-Entry Systems Operation, Aerodynamics Laboratory. Member AIAA.

† Specialist, Re-Entry Systems Operation, Aerodynamics Laboratory.

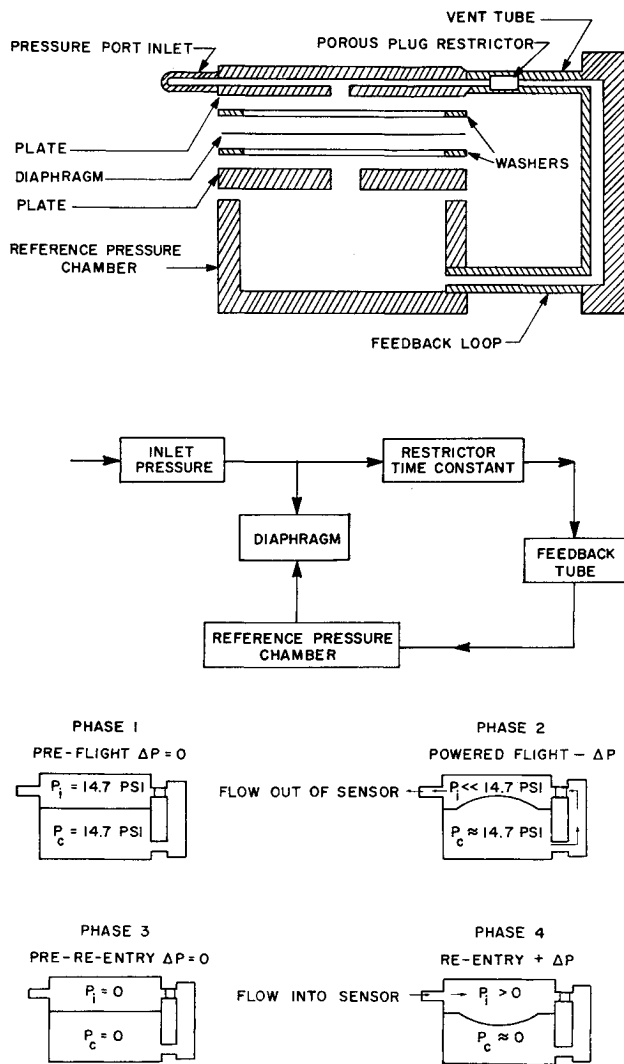


Fig. 1 Schematic and block diagram of a differential pressure sensor with a time constant.

before launch; hence the pressure differential ( $\Delta p$ ) is zero. During the powered flight phase ( $0 < t < 90$  sec), the pressure in the calibration chamber vents, causing a flow out of the sensor and an upward deflection of the diaphragm (Fig. 1), and hence a negative  $\Delta p$ . The  $\Delta p$  falls to zero for the "pre-re-entry" phase. During the brief re-entry phase ( $330 < t < 340$  sec), the restrictor vent tube restricts the flow of high-pressure air to the calibration side (the diaphragm deflects down due to a positive  $\Delta p$ ) and the data are obtained before any appreciable rise in the reference-side pressure occurs.

Figure 3 shows two comparisons of the prototype pressure sensor output with that of a standard off-the-shelf absolute unit during simulated re-entry pressure histories; agreement is

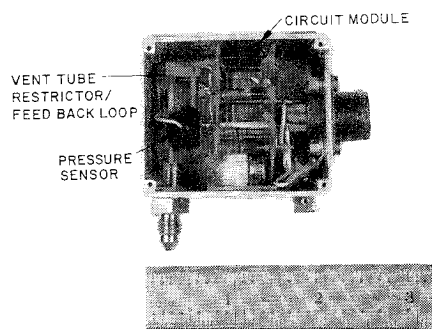


Fig. 2 GE flight prototype capacitance pressure sensor, range 0-0.2 psid, input 28 v d.c., output 50 mv d.c.

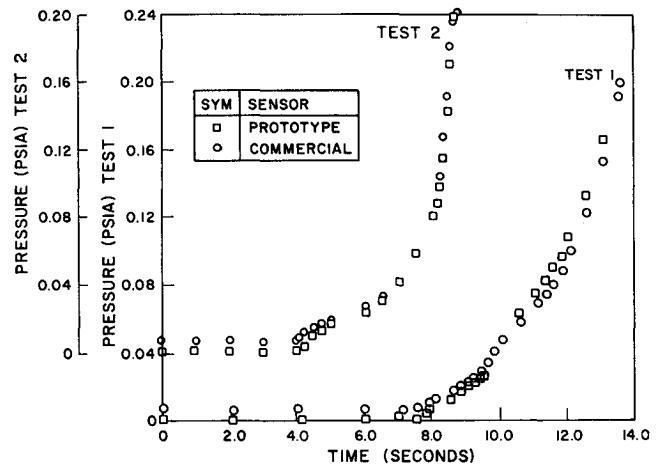


Fig. 3 Comparison of prototype sensor's readings with those of a commercial absolute pressure transducer during re-entry pressure simulation.

good, except that the absolute unit has a pre-re-entry bias of  $p \approx 0.005$  psia, probably due to calibration chamber leakage. The differential prototype sensor does not experience this classic problem because of its mode of operation.

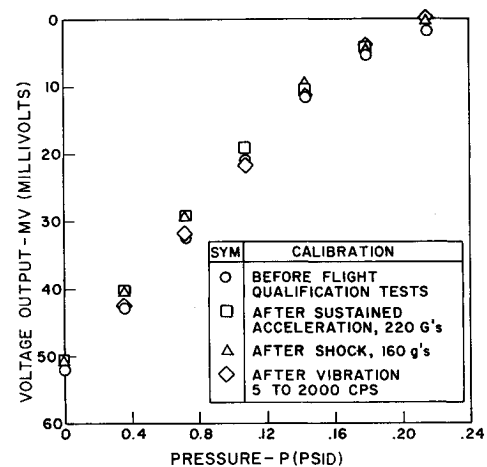


Fig. 4 Calibration curves for prototype sensor before and after flight qualification tests.

Tests were performed to determine whether a shock-tunnel-type transducer could function properly after experiencing flight environments. The prototype experienced sustained acceleration, shock, and vibration in three mutually perpendicular

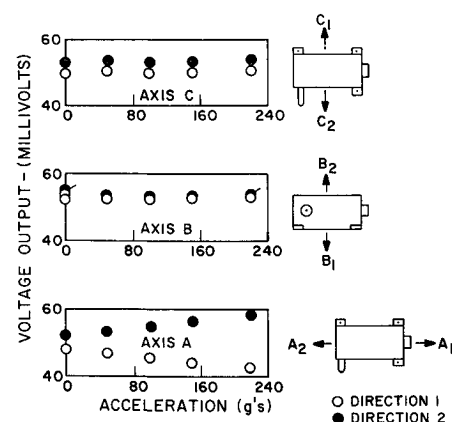


Fig. 5 Prototype sensor outputs under sustained flight qualification acceleration loads.

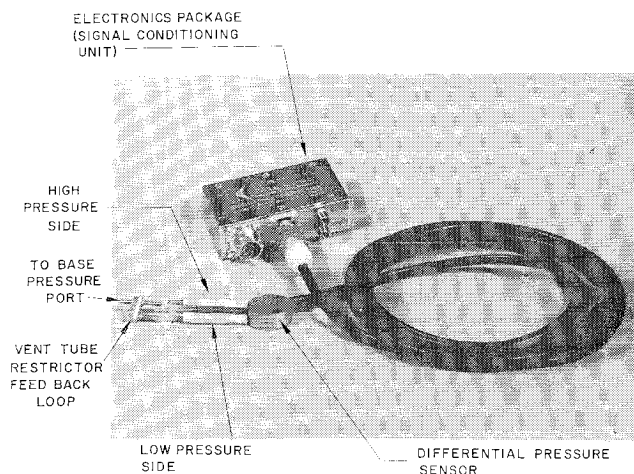


Fig. 6 Commercial differential sensor retrofitted with vent tube restrictor time constant.

ular axes. Calibration shifts were acceptably small (Fig. 4). Another test was made to simulate sustained deceleration of  $220 g$ 's such as would be experienced during re-entry. Figure 5 shows results for three orthogonal axes. There is not appreciable change in output voltage for axes C and B, which represent planes parallel to the diaphragm of the transducer, but in the plane perpendicular to the diaphragm (axis A), the output voltage changed by 13%. Therefore, the unit should be mounted such that the maximum loads during re-entry will occur in the plane parallel to the diaphragm.

Finally, a commercial differential sensor was retrofitted with a vent tube restrictor (Fig. 6), and re-entry pressure simulation test results were compared with those from a commercial absolute sensor. The results were good (Fig. 7).

#### Concluding Remarks

The concept of using a shock-tunnel-type differential sensor with a time constant to obtain low-level base-pressure measurements in re-entry vehicles has been demonstrated in ground tests with a flight prototype unit. This unit also successfully withstood the flight qualification environments of sustained acceleration, shock, and vibration with no degradation in calibration. A commercial differential sensor retrofitted with a vent tube restrictor agreed well with a commercial absolute sensor in other ground tests. Thus, a smaller and lighter flight package for base pressure measurements on re-entry test vehicles can be provided with no degradation in performance.

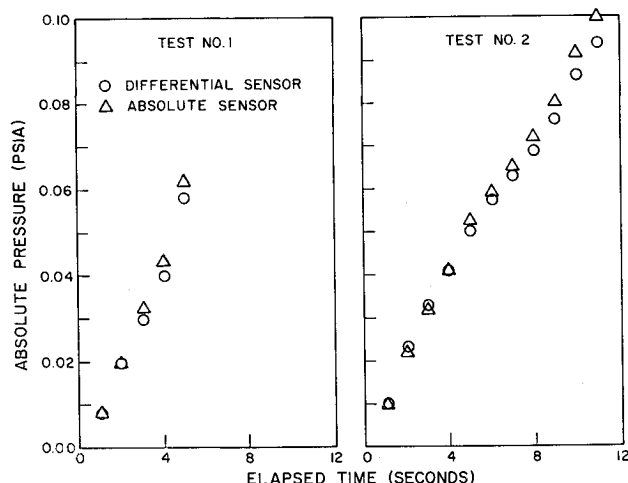


Fig. 7 Comparison of retrofitted commercial differential sensor's readings with those of a commercial absolute pressure transducer during re-entry pressure simulation.

#### References

- <sup>1</sup> Cassanto, J. M., "A New Concept for Low Range Pressure Measurements on Full Scale Flight Re-entry Vehicles," GE MSD TIS 69 SD 233, March 1969, Missile and Space Div., General Electric Co.
- <sup>2</sup> Cassanto, J. M., "Base Pressure Results at  $M \approx 12$  Utilizing Free Flight Telemetry Techniques on the GE MSD Long Test Time Facility," GE MSD ATDM 66-24, Missile and Space Div., General Electric Co.
- <sup>3</sup> Ward, L. K. and Choate, R. H., "A Model Drop Technique for Free Flight Measurements in Hypersonic Wind Tunnels Using Telemetry," AEDC-TR-66-77, May 1966, Arnold Engineering Development Center, Tullahoma, Tenn.
- <sup>4</sup> Welton, J. T., "Free-Flight Testing in the Jet Propulsion Laboratory Wind Tunnels," TR 32-775, Sept. 1965, Jet Propulsion Lab., Pasadena, Calif.

## Manned Maintenance and Refueling in Near and Deep Space Logistics

ROBERT J. SALKELD\*  
Los Angeles, Calif.

#### Nomenclature

- $C$  = sum of annual logistic ( $C_l$ ) and amortized (acquisition + deployment,  $C_{a/d}$ ) cost per mission payload
- $C_b$  = boost cost per pound of payload in orbit
- $C_p$  = acquisition cost per pound for mission payload
- $C_s$  = acquisition cost per pound for station and associated equipment
- $g$  = gravitational acceleration,  $32.2 \text{ ft/sec}^2$
- $I$  = specific impulse, sec
- $K$  = (stage gross wt/stage payload) ratio,  $w_o/w_p = (r - 1)/(1 - \lambda r)$
- $l$  = station crew duty cycle
- $n_o$  = number of shuttle flights to rotate one station crew
- $n_m$  = number of payloads serviced per earth-based flight
- $n_s$  = number of payloads serviced from one station
- $R$  = reliability for a launch-transit rendezvous
- $r$  = vehicle gross weight/burnout weight
- $T$  = time from initial system operation
- $t$  = mean time between failures for unattended payload
- $w$  = weight
- $\alpha$  = large payload boost cost parameter [boost cost per pound in near orbit for large payload/boost cost per pound in near orbit for nominal ( $\sim 25,000 \text{ lb}$ ) payload]
- $\Delta v_1$  = ideal velocity gain required for launch-transit rendezvous between near-orbit injection and single refueling, or between first and second tankers
- $\Delta v_2$  = ideal velocity gain required after final refueling, for mission maneuvers (e.g., altitude change from near to far orbit) and return to aerodynamic re-entry
- $\Delta v_3$  = ideal velocity gain required after mission maneuvers to return truck and manned shuttle to near orbit
- $\lambda$  = stage structure factor,  $w_{str}/(w_{pr} + w_{str})$
- $\tau$  =  $t/(\text{service cycle maintained})$

#### Subscripts

- $DF$  = direct flight
- $DR, SR$  = double refueling and single refueling, respectively
- $EB, SB$  = earth-based and station-based, respectively
- $MT$  = maneuvering truck
- $TR$  = total replacement
- $g$  = stage gross

Received April 18, 1969; revision received July 8, 1969. The author wishes to thank B. P. Leonard, The Aerospace Corporation, for his contribution to the methodology for comparing maintenance modes.

\* Consultant, 410 $\frac{1}{2}$  Landfair Avenue, Westwood Village. Member AIAA.